Intensity characteristics of inversionless lasers from induced atomic coherence

Yifu Zhu,[1] Min Xiao,[2] and Yang Zhao[3]
[1]Department of Physics, Florida International University, Miami, Florida 33199
[2]Department of Physics, University of Arkansas, Fayetteville, Arkansas 72701
[3]Department of Electrical and Computer Engineering, Wayne State University, Detroit, Michigan 48202
(Received 1 November 1993)

We analyze a laser system consisting of N closed three-level atoms confined in a single-mode cavity and derive the conditions for the onset of lasing without inversion or with inversion. We calculate the steady-state gain and lasing in the system and show that far above the lasing threshold, depending on the pumping and decay rates, the inversionless laser may operate in three different regimes, where the intensity of the laser depends linearly on N, is proportional to $\sqrt{N}$, or independent of N.

PACS number(s): 42.55.−f, 42.50.Hz, 32.80.Bx

I. INTRODUCTION

The optical gain and lasing without the requirement of population inversion has been the subject of much interest recently. Light amplification without inversion can be induced by optical coherence among the coupled states driven by laser fields, or by the difference between the absorption and emission paths manifested by quantum interference. Many models have been proposed, and the conditions for the onset of lasing action have been examined [1–7]. The concept of lasing without inversion (LWI) may be useful in the generation of coherent radiations in the wavelength regime where lasing with population inversion is difficult to achieve by conventional pumping mechanisms. It has been shown that the optical coherence and quantum interference associated with the light amplification may lead to novel statistical properties in inversionless lasers, such as reduced laser linewidth and amplitude squeezing [8–11]. Recently, light amplification without population inversion in the transient regime has been observed experimentally by several groups [12–15]. In general, the mechanism of LWI depends on the specific model [7], and particularly, the context of noninversion depends on the specific state basis. In atomic systems driven by external coherent fields, one can find model systems where there is no population inversion in the bare atomic states, but there is population inversion in the dressed states (for example, a strongly driven two-level system [16]). Nevertheless, a few model systems have been shown to exhibit lasing without inversion in any state basis [17,18].

Here we present an analysis of a laser model (see Fig. 1) that consists of an ensemble of N closed three-level atoms incoherently pumped to the upper state $|3\rangle$, and a coherent field drives the transition between states $|1\rangle$ and $|2\rangle$. Lasing occurs from state $|3\rangle$ to state $|2\rangle$. Similar three-level systems have been treated by Fleischhauer *et al.* [19], where the enhanced refractive index without absorption via atomic coherences was analyzed. Here the steady-state gain and lasing will be analyzed. We show that depending on the pumping and decay parameters, this three-level system may exhibit lasing with inversion or LWI (light amplification by coherence), so it serves as a model for both a conventional laser and an inversionless laser. Also, the system may demonstrate a transition from lasing with inversion to LWI [11], indicating that such a transition is common in a coherent driven laser system. Well above the threshold, the intensity of this inversionless laser may show different functional dependence on the total atomic number N, which is correlated to the specific population distributions.

The paper is organized as follows. In Sec. II, we will derive the system Hamiltonian and the semiclassical laser equations of motion. In Sec. III, we derive the conditions for the existence of gain in the system with or without population inversion. In Sec. IV, we discuss the steady-state lasing for the resonant excitation and present calculations for the threshold condition, the lasing intensity, and population distributions above the threshold. In the limit of a large atomic number N, we show that the laser intensity dependence on N is determined by the lasing mechanisms. In Sec. V, we summarize our calculations and discuss the experimental feasibility for the model system.

II. THREE-LEVEL LASER MODEL

Our model consists of an ensemble of N closed three-level atoms confined in a single-mode cavity with photon loss rate 2κ at the output port. The atoms have ground state $|1\rangle$, and excited states $|2\rangle$ and $|3\rangle$ as illustrated in Fig. 1. The excited state $|3\rangle$ is populated from the ground state $|1\rangle$ by incoherent pumping with a rate Λ. The transition $|1\rangle\leftrightarrow|2\rangle$ of frequency ω_{21} is driven by a laser of frequency ω_1 with Rabi frequency 2Ω. g is the single atom-cavity coupling coefficient on the lasing transition $|3\rangle\leftrightarrow|2\rangle$. γ_{ij} $(i,j=1-3)$ is the spontaneous decay rate from state $|i\rangle$ to state $|j\rangle$. We treat classically the external coherent field which drives the transition $|1\rangle\leftrightarrow|2\rangle$, but keep the cavity field quantized. For the convenience of the calculation, Ω and g are chosen to be real. In the dipole approximation, the system Hamiltonian can be written as

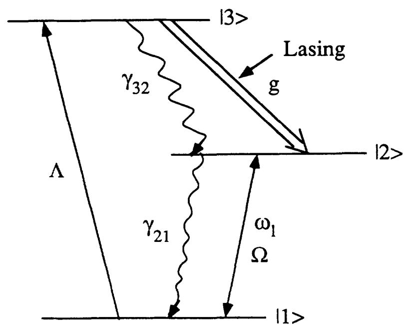

FIG. 1. Three-level model for lasing without or with population inversion. $|3\rangle \rightarrow |2\rangle$ is the lasing transition.

$$\hat{H} = \omega_{31}\hat{J}_{33} + \omega_{21}\hat{J}_{22} + \Omega(e^{-i\omega_1 t}\hat{J}_{21} + e^{i\omega_1 t}\hat{J}_{12}) + g(\hat{a}\hat{J}_{32} + \hat{a}^{\dagger}\hat{J}_{23}) + \omega_c \hat{a}^{\dagger}\hat{a} \ , \tag{1}$$

where

$$\hat{J}_{12} = \sum_{j=1}^{N} e^{-i\mathbf{k}_c\cdot\mathbf{r}_j}|1_j\rangle\langle 2_j| \ ,$$

$$\hat{J}_{13} = \sum_{j=1}^{N} e^{-i(\mathbf{k}_1+\mathbf{k}_c)\cdot\mathbf{r}_j}|1_j\rangle\langle 3_j| \ ,$$

$$\hat{J}_{23} = \sum_{j=1}^{N} e^{-i\mathbf{k}_c\cdot\mathbf{r}_j}|2_j\rangle\langle 3_j| \ ,$$

$$\hat{J}_{ll} = \sum_{j=1}^{N} |l_j\rangle\langle l_j| \quad (l=1\text{–}3) \ .$$

Here $\hat{J}_{ij}$ are the collective atomic raising or lowering operators and $\hat{J}_{ll}$ are the population operators. $\mathbf{k}_1(\mathbf{k}_c)$ is the k vector of the external driving field (cavity field). $\hat{a}(\hat{a}^{\dagger})$ is the annihilation (creation) operator for the cavity photons. ω_{ij} is the transition frequency from state $|i\rangle$ to state $|j\rangle$. To study the steady-state gain and lasing in this system, we only need the semiclassical equations of motion for the expectation values of operators. On transforming to the appropriate rotating frame, we obtain the semiclassical laser equations as follows:

$$\dot{J}_{11} = -\Lambda J_{11} + \gamma_{21}J_{22} - i\Omega(J_{12} - J_{21}) \ ,$$

$$\dot{J}_{33} = \Lambda J_{11} - \gamma_{32}J_{33} + ig(a^{*}J_{23} - aJ_{32}) \ ,$$

$$\dot{J}_{12} = -\left[\frac{\gamma_{21}+\Lambda}{2} + i\Delta_1\right]J_{12} - i\Omega(J_{11} - J_{22}) - iga^{*}J_{13} \ ,$$

$$\dot{J}_{13} = -\left[\frac{\gamma_{32}+\Lambda}{2} + i(\Delta+\Delta_1)\right]J_{13} + i\Omega J_{23} - iga^{*}J_{12} \ , \tag{2}$$

$$\dot{J}_{23} = -\left[\frac{\gamma_{32}+\gamma_{21}}{2} + i\Delta\right]J_{23} - iga(J_{22} - J_{33}) + i\Omega J_{13} \ ,$$

$$\dot{a} = -[\kappa + i(\omega_c - \omega_l)]a - igJ_{23} \ ,$$

together with the equations of their complex conjugates. In Eqs. (2), $\Delta = \omega_{32} - \omega_l$, and $\Delta_1 = \omega_{21} - \omega_1$. Above the threshold, ω_l is the lasing frequency. Since the system is closed, we have $J_{11} + J_{22} + J_{33} = N$. Setting the derivatives in Eqs. (2) to zero, the steady-state laser intensity and atomic population distributions can be obtained. The gain coefficient for the cavity field coupled to the transition $|3\rangle \rightarrow |2\rangle$ is proportional to $\mathrm{Im}(J_{23})$. If $\mathrm{Im}(J_{23}) > 0$, the system exhibits gain for the cavity field, and lasing can be established on the transition $|3\rangle \rightarrow |2\rangle$ if the gain is larger than the cavity loss. First, assuming the cavity field can be treated as a weak, classical coherent field, we analyze the dependence of the optical gain on various system parameters. For the resonant excitations, i.e., $\Delta = \Delta_1 = 0$, we present simple analytical expressions for the gain coefficient $\mathrm{Im}(J_{23})$ and the population distributions, from which it is easy to derive the conditions for the onset of LWI or lasing with inversion. For the off-resonant excitation $\Delta_1 = 0$ we show that the probe gain may occur at one or both Rabi sidebands, which can be viewed as due to population inversion in the dressed states. Second, we discuss the steady-state lasing in the system and present calculations for the threshold condition, the laser intensity, and population distributions. From the analytical results in the limit of $\sqrt{N}g \gg \Omega$, γ_{ij}, and Λ, and numerical calculations under various operating conditions, we show that the light amplification mechanism can be inferred from the observation of the laser intensity dependence on N.

III. STEADY-STATE GAIN AND POPULATION DISTRIBUTIONS

Replacing the cavity field by a weak, coherent probe field, we set ga and ga^{*} in Eqs. (2) equal to g, where $2g$ is the Rabi frequency of the probe field. Setting the derivatives in Eqs. (2) to zero, it is easy to obtain the analytical expressions for the probe gain coefficient $\mathrm{Im}(J_{23})$ and population distributions J_{ii} $(i=1,3)$ in the steady state. These expressions are quite tedious, so it is difficult to extract essential physics from them. Therefore we have opted to present analytical results under the resonant excitation, $\Delta_1 = \Delta = 0$, and in the limit of a strong coherent field such that $\Omega \gg \gamma_{ij}$, g, and Λ. With such an approximation, we obtain

$$\mathrm{Im}(J_{23}) = \frac{Ng(\Lambda^2 + \Lambda\gamma_{32} - \gamma_{32}^2 - \gamma_{21}\gamma_{32})}{2\Omega^2(\Lambda + 2\gamma_{32})} \ , \tag{3}$$

and $\mathrm{Re}(J_{23}) = 0$. The weak probe field is amplified at the frequency $\omega_l = \omega_{32}$ if the incoherent pumping rate satisfies $\Lambda > \sqrt{\gamma_{32}^2/4 + \gamma_{32}(\gamma_{32}+\gamma_{21})} - \gamma_{32}/2$. Similarly, the population distributions can be readily derived. They are

$$J_{11} = J_{22} = \frac{\gamma_{32}N}{\Lambda + 2\gamma_{32}} \tag{4}$$

and

$$J_{33} = \frac{\Lambda N}{\Lambda + 2\gamma_{32}} \ . \tag{5}$$

Combining the requirements for the existence of gain and

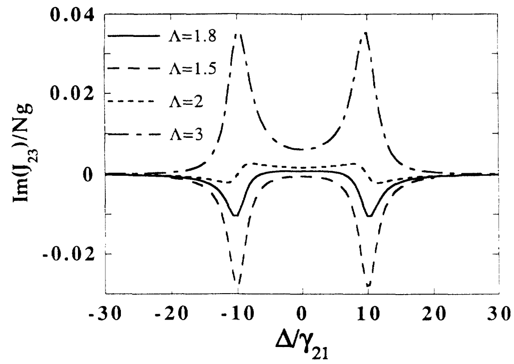

FIG. 2. Calculated steady-state gain $\mathrm{Im}(J_{23})$ vs Δ/γ_{21} for four sets of Λ values with $\Delta_1=0$, $\gamma_{32}=2$, $\Omega=10$, and $g=0.001$ (in γ_{34} units). Gain without population inversion exists for $\Lambda=2$ and 1.8. For $\Lambda=1.5$, there is no gain. When $\Lambda>2$, gain is due to population inversion. Notice the constructive interference at the line center $\Delta=0$.

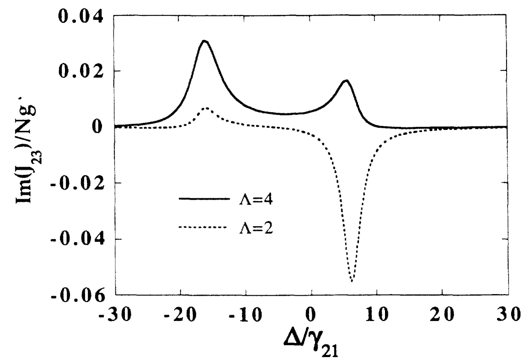

FIG. 3. Calculated steady-state gain $\mathrm{Im}(J_{23})$ vs Δ/γ_{21} for two sets of Λ values with $\Delta_1=10$, $\gamma_{32}=2$, $\Omega=10$, and $g=0.001$ (in γ_{34} units). For $\Lambda=2$, there is no population inversion in the bare atomic states. The gain peak at $\Delta=-\Delta_1/2-\sqrt{\Delta_1^2/4+\Omega^2}$ is due to the population inversion between the state $|3\rangle$ and the dressed state $|-\rangle$. When $\Lambda=4$, there is population inversion in both the bare atomic states and the dressed states, so the gain appears at both transition frequencies of Autler-Towne's doublet, $\Delta=-\Delta_1/2\pm\sqrt{\Delta_1^2/4+\Omega^2}$.

population noninversion, the sufficient and necessary condition for the system to exhibit LWI is

$$\gamma_{32}>\Lambda>\left[\frac{\gamma_{32}^2}{4}+\gamma_{32}(\gamma_{32}+\gamma_{21})\right]^{1/2}-\frac{\gamma_{32}}{2}\,. \tag{6}$$

On the other hand, the condition for the onset of lasing with inversion is

$$\Lambda>\gamma_{32},\quad \Lambda>\left[\frac{\gamma_{32}^2}{4}+\gamma_{32}(\gamma_{32}+\gamma_{21})\right]^{1/2}-\frac{\gamma_{32}}{2}\,. \tag{7}$$

To examine the general characteristics of gain in the model system, we present numerical calculations of $\mathrm{Im}(J_{23})$ versus the probe detuning Δ for several sets of Λ values (normalized by γ_{21}) with the other parameters chosen as $\Delta_1=0$, $\gamma_{32}=2\gamma_{21}$, $\Omega=10\gamma_{21}$, $g=10^{-3}\gamma_{21}$. The coherent driving field generates a pair of dressed states ($|+\rangle$ and $|-\rangle$) that are separated by the Rabi frequency 2Ω [20]. The probe gain profile is shown in Fig. 2. The peaks at $\Delta=\pm\Omega$ correspond to the dressed-state transitions (positive peaks represent gain while negative peaks represent absorption). For weak incoherent pumping (for example, the curve for $\Lambda=1.5$), no gain exists for the probe field. Gain without population inversion occurs for intermediate Λ values, as shown by the curves for $\Lambda=1.8$ and 2. Since there is no population inversion, gain occurs at a region centered around $\Delta=0$ and absorption is peaked at the frequencies corresponding to the dressed state transitions. The constructive interference for the transition amplitudes at $\Delta=0$ enhances the gain. At sufficiently large incoherent pumping, population inversion is created, and gain is much larger and peaked at both the dressed-state transitions $\Delta=\pm\Omega$. When the coherent driving field is off resonance, i.e., $\Delta_1\neq0$, the dressed states are polarized, or there is population imbalance among the two dressed states [20]. As the incoherent pumping rate Λ increases, population inversion can be first realized in one set of the dressed-state transitions, then the other set for still larger Λ values. For example, as shown in Fig. 3, for $\Delta_1=\Omega=10\gamma_{21}$, the upper dressed state $|+\rangle$ with higher energy is more heavily populated while the lower dressed state $|-\rangle$ is less populated. With $\Lambda=2\gamma_{21}$ the population distributions satisfy $J_{++}>J_{33}>J_{--}$, so the probe gain appears at the transition $|3\rangle\rightarrow|-\rangle$ while the dominant absorption peak occurs at the transition from $|+\rangle\rightarrow|3\rangle$. For a sufficiently large Λ, population inversion for both dressed-state transitions can be realized ($J_{33}>J_{++}>J_{--}$), and lasing can occur at both transition frequencies as shown by the curve for $\Lambda=4$.

IV. STEADY-STATE LASING ABOVE THE THRESHOLD

To study the threshold condition, the steady-state laser intensity, and population distributions above the threshold, we need to solve the semiclassical laser equations (2) with a variable cavity field. We have chosen to carry out the calculations under the conditions of resonant excitations, i.e., $\Delta=\Delta_1=0$. When the cavity is tuned to the resonant frequency of the transition $|3\rangle\rightarrow|2\rangle$, the lasing frequency $\omega_l=\omega_c=\omega_{32}$, because the dispersive response $\mathrm{Re}(J_{23})$ vanishes. The steady-state laser intensity is

$$I\equiv ng^2=\frac{-B+\sqrt{B^2-4AC}}{2A}\,, \tag{8}$$

where

$$A=\frac{2\kappa(2\Lambda+\gamma_{21})}{g^2(2\Lambda^2+4\Lambda\gamma_{32}+\Lambda\gamma_{21}+\gamma_{32}^2+\gamma_{32}\gamma_{21})},$$

$$B=\frac{Ng^2\Lambda(\gamma_{32}-\gamma_{21})}{(2\Lambda^2+4\Lambda\gamma_{32}+\Lambda\gamma_{21}+\gamma_{32}^2+\gamma_{32}\gamma_{21})}+\frac{\kappa\{2\Lambda^3+\Lambda^2(2\gamma_{32}+3\gamma_{21})+\Lambda(5\gamma_{32}\gamma_{21}+\gamma_{32}^2+2\gamma_{21}^2)\}}{2(2\Lambda^2+4\Lambda\gamma_{32}+\Lambda\gamma_{21}+\gamma_{32}^2+\gamma_{32}\gamma_{21})}$$
$$+\frac{\kappa\{\gamma_{32}\gamma_{21}(2\gamma_{21}+\gamma_{32})+4\Omega^2(2\gamma_{32}+\gamma_{21})\}}{2\{2\Lambda^2+4\Lambda\gamma_{32}+\Lambda\gamma_{21}+\gamma_{32}^2+\gamma_{32}\gamma_{21}\}},$$

$$C=-\frac{Ng^2\{4\Omega^2[\gamma_{32}(\gamma_{32}+\gamma_{21}-\Lambda)-\Lambda^2]+\Lambda(\gamma_{32}+\Lambda)(\Lambda+\gamma_{21})(\gamma_{32}-\gamma_{21})\}}{4(2\Lambda^2+4\Lambda\gamma_{32}+\Lambda\gamma_{21}+\gamma_{32}^2+\gamma_{32}\gamma_{21})}$$
$$+\frac{\kappa\{(\gamma_{32}+\gamma_{21})(\gamma_{32}+\Lambda)+4\Omega^2\}\{4\Omega^2(\Lambda+2\gamma_{32})+(\gamma_{21}+\Lambda)[(\gamma_{32}+\Lambda)(\gamma_{21}+\Lambda)-\Lambda^2]\}}{8(2\Lambda^2+4\Lambda\gamma_{32}+\Lambda\gamma_{21}+\gamma_{32}^2+\gamma_{32}\gamma_{21})}.$$

Here we define the laser intensity $I=ng^2$ where n is the number of photons inside the cavity. If we refer to $G=Ng^2$ as the atomic pumping parameter, then the laser threshold can be determined from Eq. (4) as

$$G_{\text{th}}=\frac{\kappa\{(\gamma_{32}+\gamma_{21})(\gamma_{32}+\Lambda)+4\Omega^2\}\{4\Omega^2(\Lambda+2\gamma_{32})+(\gamma_{21}+\Lambda)[(\gamma_{32}+\Lambda)(\gamma_{21}+\Lambda)-\Lambda^2]\}}{4\Omega^2[\Lambda^2-\gamma_{32}(\gamma_{32}+\gamma_{21}-\Lambda)]-\Lambda(\gamma_{32}+\Lambda)(\Lambda+\gamma_{21})(\gamma_{32}-\gamma_{21})}. \tag{9}$$

In the limit of $\sqrt{G}\gg\Omega$, γ_{ij} $(i,j=1-3)$, and Λ, it is easy to derive the laser intensity and population distributions. We found that depending on the population distributions, the laser may operate in three different regimes. First, for $\gamma_{32}>\gamma_{21}$, the population distributions are

$$J_{33}=\frac{\Lambda(\Lambda+\gamma_{21}+\gamma_{32})N}{2\Lambda^2+4\Lambda\gamma_{32}+\Lambda\gamma_{21}+\gamma_{32}^2+\gamma_{32}\gamma_{21}}, \tag{10}$$

$$J_{22}=\frac{\Lambda(\Lambda+2\gamma_{32})N}{2\Lambda^2+4\Lambda\gamma_{32}+\Lambda\gamma_{21}+\gamma_{32}^2+\gamma_{32}\gamma_{21}}, \tag{11}$$

$$J_{11}=\frac{\gamma_{32}(\Lambda+\gamma_{21}+\gamma_{32})N}{2\Lambda^2+4\Lambda\gamma_{32}+\Lambda\gamma_{21}+\gamma_{32}^2+\gamma_{32}\gamma_{21}}. \tag{12}$$

$J_{33}<J_{22}$ is always valid; there is no population inversion. The laser intensity is

$$I\equiv ng^2=\frac{\Omega^2(\Lambda^2+\Lambda\gamma_{32}-\gamma_{32}^2-\gamma_{32}\gamma_{21})}{\Lambda(\gamma_{32}-\gamma_{21})}. \tag{13}$$

The laser is saturated at high atomic pumping, and the saturation intensity is proportional to the intensity of the external coherent driving field. Second, if $\gamma_{32}=\gamma_{21}$, the population distributions are

$$J_{33}=\frac{N\Lambda(\gamma_{21}+\gamma_{32}+\Lambda)}{2\Lambda^2+4\Lambda\gamma_{32}+\Lambda\gamma_{21}+\gamma_{32}^2+\gamma_{32}\gamma_{21}}-\frac{2\kappa(2\Lambda+\gamma_{32}+\gamma_{21})}{2\Lambda^2+4\Lambda\gamma_{32}+\Lambda\gamma_{21}+\gamma_{32}^2+\gamma_{32}\gamma_{21}}\left[\frac{N\Omega^2(\Lambda^2+\Lambda\gamma_{32}-\gamma_{32}^2-\gamma_{32}\gamma_{21})}{2g^2\kappa(2\Lambda+\gamma_{21})}\right]^{1/2}, \tag{14}$$

$$J_{22}=J_{33}+\frac{2\kappa(2\Lambda+\gamma_{21})}{2\Lambda^2+4\Lambda\gamma_{32}+\Lambda\gamma_{21}+\gamma_{32}^2+\gamma_{32}\gamma_{21}}\left[\frac{N\Omega^2(\Lambda^2+\Lambda\gamma_{32}-\gamma_{32}^2-\gamma_{32}\gamma_{21})}{2g^2\kappa(2\Lambda+\gamma_{21})}\right]^{1/2}. \tag{15}$$

$J_{33}<J_{22}$; there is no population inversion. We obtain the laser intensity as follows:

$$I\equiv ng^2\left[\frac{N\Omega^2g^2(\Lambda^2+\Lambda\gamma_{32}-\gamma_{32}^2-\gamma_{32}\gamma_{21})}{2\kappa(2\Lambda+\gamma_{21})}\right]^{1/2}. \tag{16}$$

I is proportional to $\sqrt{G}$, and no saturation can be observed. Finally, if $\gamma_{32}<\gamma_{21}$,

$$J_{33}=\frac{\Lambda(2\Lambda^2+4\Lambda\gamma_{32}+\Lambda\gamma_{21}+\gamma_{32}^2+\gamma_{32}\gamma_{21})}{(2\Lambda+\gamma_{21})(2\Lambda^2+4\Lambda\gamma_{32}+\Lambda\gamma_{21}+\gamma_{32}^2+\gamma_{32}\gamma_{21})}-\frac{2\kappa(2\Lambda+\gamma_{32}+\gamma_{21})n_1}{2\Lambda^2+4\Lambda\gamma_{32}+\Lambda\gamma_{21}+\gamma_{32}^2+\gamma_{32}\gamma_{21}}, \tag{17}$$

$$J_{22}=J_{33}+\frac{2\kappa(2\Lambda+\gamma_{21})n_1}{2\Lambda^2+4\Lambda\gamma_{32}+\Lambda\gamma_{21}+\gamma_{32}^2+\gamma_{32}\gamma_{21}}, \tag{18}$$

where

$$n_1=\frac{\Omega^2[2\Lambda^3+\Lambda(\Lambda-\gamma_{21})(\gamma_{21}+2\gamma_{32})-\gamma_{32}\gamma_{21}(\gamma_{32}+\gamma_{21})\}}{\Lambda g^2(\gamma_{21}-\gamma_{32})(2\Lambda+\gamma_{21})}-\frac{(\gamma_{32}+\gamma_{21})(\gamma_{32}\gamma_{21}+\Lambda\gamma_{32}+\Lambda\gamma_{21})}{4g^2(2\Lambda+\gamma_{21})} .$$

The laser intensity becomes

$$I\equiv ng^2=\frac{Ng^2\Lambda(\gamma_{21}-\gamma_{32})}{2\kappa(2\Lambda+\gamma_{21})}+n_1g^2 . \tag{19}$$

It is interesting to note that whether there is population inversion or noninversion is determined by the strength of coherent pump field. For a strong coherent field such that

$$\Omega^2\geq\frac{\Lambda(\gamma_{21}-\gamma_{32})(\gamma_{32}+\gamma_{21})(\gamma_{32}\gamma_{21}+\Lambda\gamma_{32}+\Lambda\gamma_{21})}{4\{2\Lambda^3+\Lambda(\Lambda-\gamma_{21})(\gamma_{21}+2\gamma_{32})-\gamma_{32}\gamma_{21}(\gamma_{32}+\gamma_{21})\}} , \tag{20}$$

there is no population inversion, lasing is maintained by the induced coherence J_{13}, and the intracavity laser intensity is proportional to N, the number of atoms in the cavity mode. When $N\gg1$, the term proportional to n_1 in population distributions is negligible, so for all practical purposes, $J_{22}=J_{33}$, the inversionless laser behaves very much like an inversion laser in this limit.

It is interesting to note that if $\gamma_{32}<\gamma_{21}$, only lasing with population inversion may be initialized in this three-level system. Then the system may maintain the lasing with persistent population inversion if the coherent field is weak or absent. On the other hand, LWI may be responsible for the laser action if the coherent pump field is strong [the inequality (20) is valid] once the laser is well above the threshold. The system will exhibit the transition from lasing with population inversion to LWI. Such a dynamic transition is quite common in a coherently pumped laser system as we have shown in other inversionless systems [11].

In order to have a complete picture of the lasing characteristics in this three-level system, we need to examine the intermediate regime between the weak lasing around the threshold and the high field limit at large G. We have carried out numerical calculations for the laser intensity and population distributions versus G in the three different operating regimes discussed above. Shown in Fig. 4 are the calculated laser intensity and population distributions as functions of the atomic pumping G for two sets of Λ values and $\gamma_{32}>\gamma_{21}$ ($\gamma_{32}=2\gamma_{21}$). The laser intensity saturates at high G values as shown in Fig. 4(a), demonstrating the characteristics of LWI in this particular system. For $\Lambda=1.8\gamma_{21}<\gamma_{32}$, there is no population inversion for arbitrary G values as shown in Fig. 4(c). However, for $\Lambda=2.5\gamma_{21}>\gamma_{32}$, lasing is initiated from population inversion near the threshold as shown in Fig. 4(b). As the atomic pumping G increases, the transition from lasing with inversion to LWI occurs, and after the transition, lasing is maintained solely by the atomic coherence. For $\gamma_{32}\leq\gamma_{21}$, the lasing can be initialized only from population inversion, which requires a sufficient strong incoherent pumping. As shown in Fig. 5, for $\gamma_{32}=\gamma_{21}$, the laser intensity is proportional to $\sqrt{G}$ at large G values while for $\gamma_{32}<\gamma_{21}$, the laser intensity linearly depends on G. In both cases, the system starts lasing from population inversion, then makes the transi-

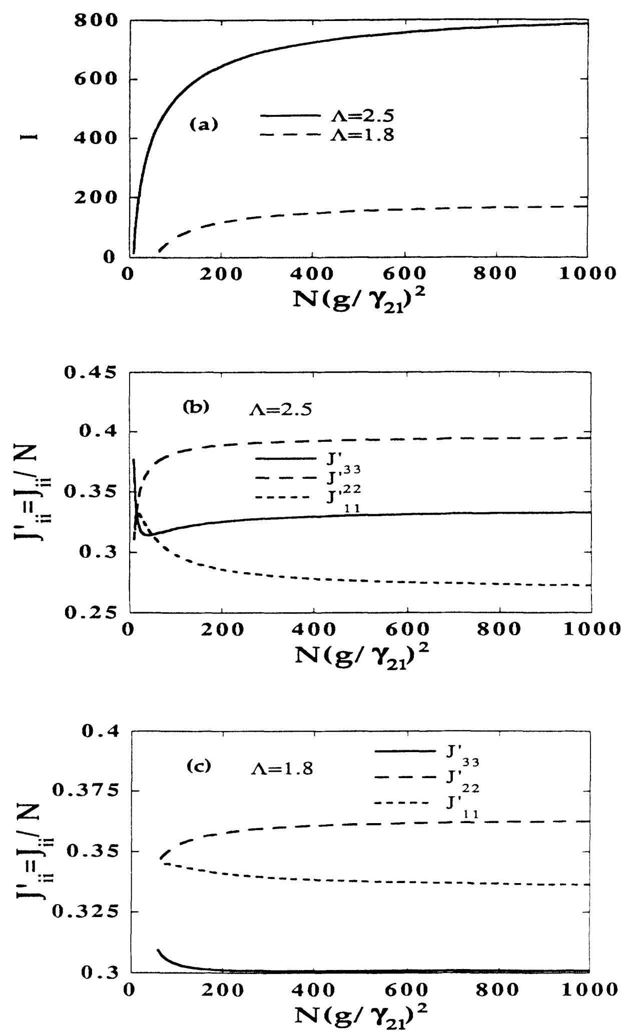

FIG. 4. (a) Calculated steady-state laser intensity $n(g/\gamma_{21})^2$ vs the atomic pumping parameter $G=N(g/\gamma_{21})^2$ for two sets of Λ values (in γ_{21} units) and $\gamma_{32}>\gamma_{21}$ (the other parameters are $\Omega=20\gamma_{21}$ and $\kappa=0.01\gamma_{21}$). Far above the threshold, the laser intensities are independent of G. (b) The normalized population distributions J'_{ii} ($i=1-3$) for $\Lambda=2.5$. Note that the initial lasing is due to population inversion, but as G increases far above the threshold value, the transition from lasing with inversion to LWI occurs. (c) The normalized population distribution J'_{ii} ($i=1-3$) for $\Lambda=1.8$. Lasing is due to light amplification by coherence for arbitrary G values.

tion to LWI. Afterwards, the lasing is maintained by the induced coherence J_{13} only; there is no population inversion ($J_{33} < J_{22}$) for arbitrary G values. In Fig. 6, we plot the laser intensity and population distributions versus the Rabi frequency of the coherent pump field Ω/γ_{21} for two sets of the incoherent pump rate Λ. G is chosen to be 1000, and the other parameters are the same as in Fig. 4. For a small Λ value (1.8), LWI is valid for all Ω values with which lasing can be maintained. But for a larger Λ value (2.5), there is a threshold Ω value below which the system exhibits LWI; above which lasing with inversion takes place in the system. It is noted that above threshold, as the coherent pumping increases from zero, the laser intensity increases, gradually reaches the maximum, and then decreases monotonically to zero. This can be understood as follows: the coherent field generates a pair of dressed states which are separated by the Rabi frequency 2Ω. Since the laser is centered at the transition ω_{32}, the large detuning from the real dressed-state transitions eventually becomes dominant as shown in Eq. (3), which diminishes the gain and raises the lasing threshold. For a fixed G value, at large Ω values, lasing at $\Delta=0$ requires increased population inversion to balance the gain reduction. Eventually, when Ω is too large, even though the population inversion can be large as shown in Fig. 6(b), the gain at $\Delta=0$ is not sufficient to sustain the laser action. It should be noted that with population inversion, the gain is peaked at both Rabi sidebands, lasing can be easily maintained at the cavity frequencies

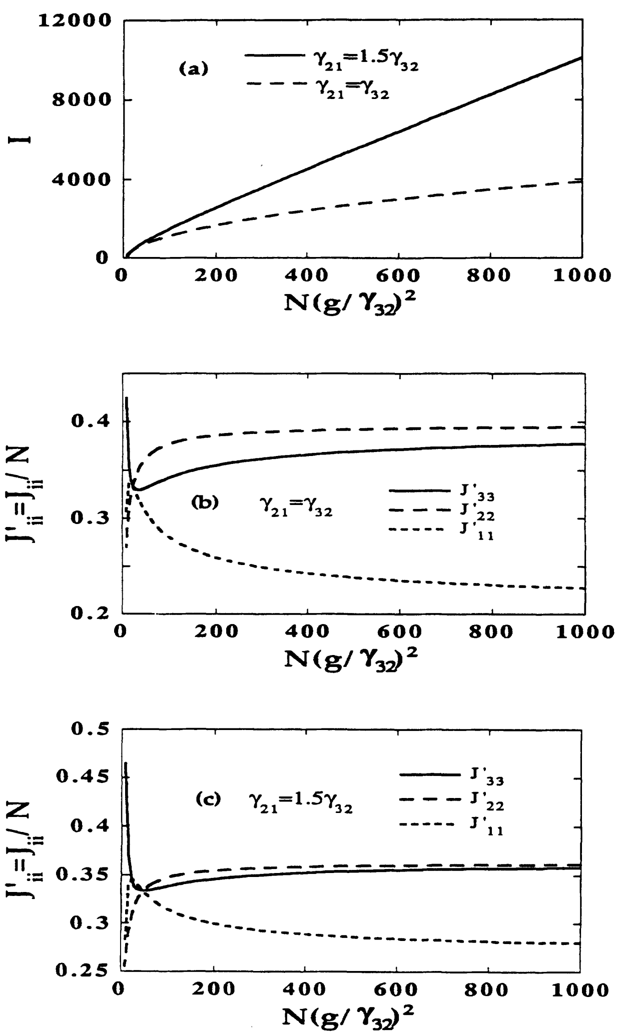

FIG. 5. (a) Calculated steady-state laser intensity $n(g/\gamma_{32})^2$ vs the atomic pumping parameter $G=N(g/\gamma_{32})^2$ for two sets of γ_{21} values ($\gamma_{32} \leq \gamma_{21}$) with $\Lambda=3\gamma_{32}$, $\Omega=20\gamma_{32}$, and $\kappa=0.01\gamma_{32}$. The laser intensity is dependent on $\sqrt{G}$ for $\gamma_{32}=\gamma_{21}$, and linearly dependent on G for $\gamma_{32}<\gamma_{21}$. (b) The normalized population distributions J'_{ii} ($i=1-3$) for $\gamma_{32}=\gamma_{21}$. (c) The normalized population distributions $J'_{ii}=(i=1-3)$ for $\gamma_{21}=2\gamma_{32}$. In both cases, $J_{22}<J_{33}$, lasing is solely due to population inversion.

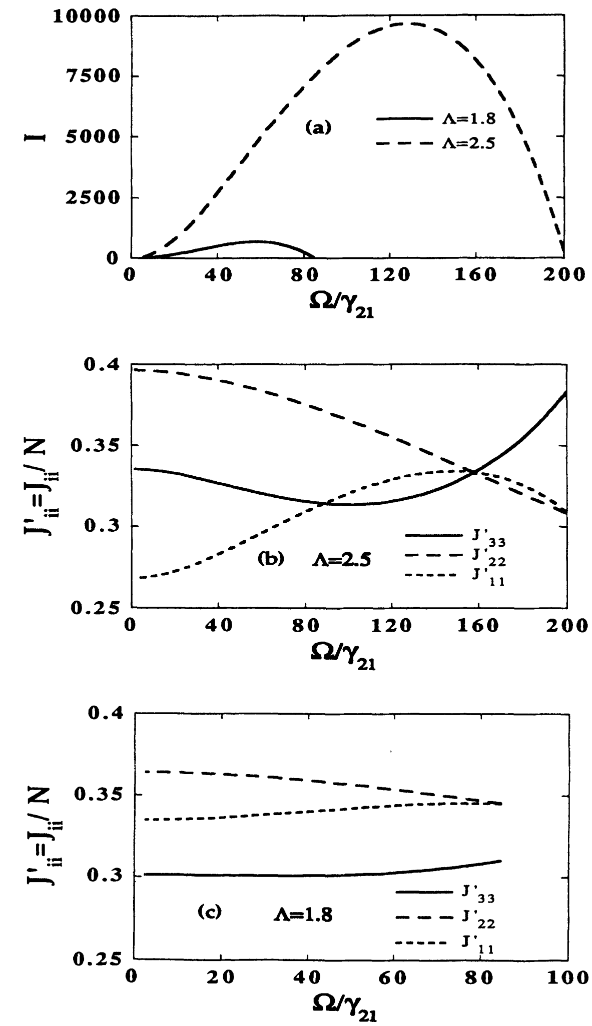

FIG. 6. (a) Calculated steady-state laser intensity $n(g/\gamma_{21})^2$ vs the normalized Rabi frequency Ω/γ_{21} for two sets of Λ values (in γ_{21} units) and $\gamma_{32}>\gamma_{21}$ (the other parameters are $\Omega=20\gamma_{21}$ and $\kappa=0.1\gamma_{21}$). As Ω increases from the threshold, the laser intensity I first increases, then reaches the maximum value, and afterwards, decreases monotonically to zero. (b) The normalized population distributions J'_{ii} ($i=1-3$) for $\Lambda=2.5$. Note that LWI is valid for $\Omega/\gamma_{21}<160$, above which lasing can only exist with population inversion. (c) The normalized population distribution J'_{ii} ($i=1-3$) for $\Lambda=1.8$. Lasing is solely due to light amplification by coherence for Ω/γ_{21} values under which I is nonzero.

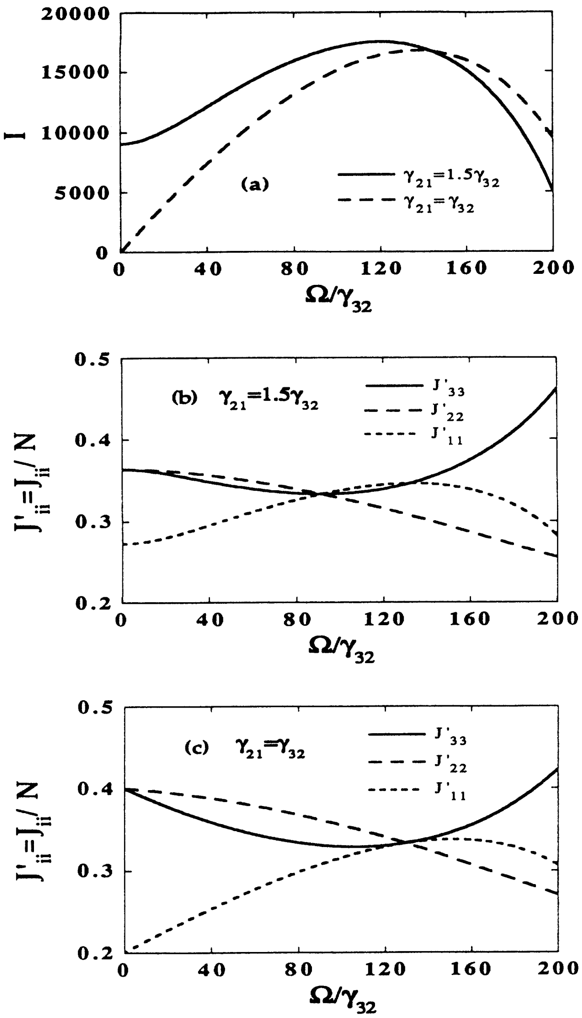

FIG. 7. (a) Calculated steady-state laser intensity $n(g/\gamma_{21})^2$ vs the normalized Rabi frequency Ω/γ_{21} for $\gamma_{32}=\gamma_{21}$ and $\gamma_{21}=1.5\gamma_{32}$ (the other parameters are $\Omega=20\gamma_{21}$, $\Lambda=2.5\gamma_{21}$, and $\kappa=0.01\gamma_{21}$). As Ω increases, the laser intensity I first increases, then reaches the maximum value, and afterwards, decreases monotonically to zero. (b) The normalized population distributions J'_{ii} $(i=1-3)$ for $\gamma_{21}=1.5\gamma_{32}$. Note that LWI is possible for intermediate Ω values; for larger or small Ω values, lasing with inversion takes place. (c) The normalized population distribution J'_{ii} $(i=1-3)$ for $\gamma_{21}=\gamma_{32}$.

$\Delta=\pm\Omega$. Plotted in Fig. 7 are the laser intensities and population inversions versus Ω/γ_{21} for $G=1000$, $\gamma_{21}=\gamma_{32}$, and $\gamma_{21}=1.5\gamma_{32}$, respectively. Λ is chosen to be $2.5\gamma_{32}$ and the other parameters are the same as in Fig. 5. For $\gamma_{21}=1.5\gamma_{32}$, lasing can be achieved in the absence of the coherent pump field, since the incoherent pump Λ is sufficient to create population inversion on the transition $|3\rangle\rightarrow|2\rangle$. For a fixed G value ($G=1000$), the laser in the steady state has three operating regimes: for small Ω values, lasing is due to population inversion; for intermediate Ω values, LWI takes place; and for large Ω values, the lasing mechanism is back to population inversion again as shown in the population distributions plotted in Fig. 7(b).

V. CONCLUSIONS

We have analyzed the gain and lasing in a closed three-level system and derived the conditions for the onset of LWI or lasing with population inversion. In particular, the model system may be made to start lasing from population inversion, and make the transition to LWI after reaching the threshold. Therefore this laser model provides another example of the dynamic transition between a conventional laser and an inversionless laser, indicating such a dynamic transition is common in a coherently pumped laser system. We have shown that an inversionless laser may exhibit quite different intensity dependence on the atomic pumping parameter $G=Ng^2$. Specifically, far above the threshold, depending on the pump and decay rates, the laser intensity from LWI may depend linearly on G, or be independent of G.

For an inhomogeneously broadened system, if the Rabi frequency 2Ω of the coherent driving field is on the order of the inhomogeneously broadened linewidth for the transition $|2\rangle\leftrightarrow|1\rangle$, the basic physical conclusions presented here will be valid. The reduced gain at a large Ω value will increase the lasing threshold, but the available number of atoms usually can be much larger (for example, in an atomic vapor system) than that of a Doppler-free system, so the laser scheme could still be realized in practice. Other factors, such as collisional dephasing, collisional excitation, and deexcitation, can be added in the population and phase decay terms in the density matrix equations. One then can solve Eqs. (2) with modified Λ and γ_{ij} parameters.

One candidate for the experimental investigation of this three-level system may be found in Ruby, where the ^2E excited states correspond to state $|3\rangle$, the magnetic sublevels $|\pm\frac{1}{2}\rangle$ of $^4A_2$ ground states correspond to state $|2\rangle$, and the sublevels $|\pm\frac{3}{2}\rangle$ of $^4A_2$ ground states correspond to state $|1\rangle$. The incoherent pumping from $|1\rangle$ to $|3\rangle$ may be realized by pumping from $^4A_2$ to $^4F_2$ (or $^4F_1$) and the subsequent fast decay from $^4F_2$ (or $^4F_1$) to ^2E states. The coherent pumping between $|1\rangle$ and $|2\rangle$ may be achieved by a microwave field of 12 to 18 GHz. Since $\gamma_{32}\gg\gamma_{21}$, the condition for LWI is satisfied. A quantitative analysis and experimental study for the proposed Ruby system are in progress.

ACKNOWLEDGMENT

One of us (Y. Zhao) acknowledges support from ONR through Grant No. N00014-93-1-0576.

[1] S. E. Harris, Phys. Rev. Lett. **62**, 1033 (1989); A. Imamoglu, Phys. Rev. A **40**, 4135 (1989); S. E. Harris and J. J. Macklin, *ibid.* **40**, 4135 (1989).
[2] M. O. Scully, S. Y. Zhu, and A. Gavrielides, Phys. Rev. Lett. **62**, 2813 (1989); E. F. Fill, M. O. Scully, and S. Y. Zhu, Opt. Commun. **77**, 36 (1990).
[3] V. G. Arkhipkin and Yu. I. Heller, Phys. Lett. **98A**, 12 (1983).

[4] G. S. Agarwal, S. Ravi, and J. Cooper, Phys. Rev. A **41**, 4721 (1990); **41**, 4727 (1990); G. B. Prasad, and G. S. Agarwal, Opt. Commun. **86**, 409 (1991).
[5] O. Koarovskaya and P. Mandel, Phys. Rev. A **42**, 523 (1990); Opt. Commun. **77**, 215 (1990).
[6] S. Basil and P. Lambropoulos, Opt. Commun. **78**, 163 (1990); A. Lyras, X. Tang, P. Lambropoulos, and J. Zhang, Phys. Rev. A **40**, 4131 (1989).
[7] L. M. Narducci, H. M. Doss, P. Ru, M. O. Scully, S. Y. Zhu, and C. H. Keitel, Opt. Commun. **81**, 379 (1991); L. M. Narducci, M. O. Scully, C. H. Keitel, S. Y. Zhu, and H. M. Doss, *ibid.* **86**, 324 (1991).
[8] G. S. Agarwal, Phys. Rev. Lett. **67**, 980 (1991).
[9] K. M. Gheri and D. F. Walls, Phys. Rev. Lett. **68**, 3428 (1992); Phys. Rev. A **45**, 6675 (1992).
[10] H. Ritsch, M. A. M. Marte, and P. Zollar, Europhys. Lett. **19**, 7 (1992); H. Ritsch and M. A. Marte, Phys. Rev. A **47**, 2354 (1993).
[11] Y. Zhu and M. Xiao, Phys. Rev. A **48**, 3895 (1993).
[12] J. Y. Gao, C. Guo, X. Z. Guo, G. X. Jin, Q. W. Wang, J. Zhao, H. Z. Zhang, Y. Jiang, W. Z. Wang, and D. M. Jiang, Opt. Commun. **93**, 323 (1992).
[13] A. Nottelman, C. Peters, and W. Lange, Phys. Rev. Lett. **70**, 1783 (1993).
[14] E. S. Fry, X. Li, D. Nikonov, G. G. Padmabandu, M. Scully, A. V. Smith, F. Tittel, C. Wang, S. R. Wilkinson, and S. Y. Zhu, Phys. Rev. Lett. **70**, 3235 (1993).
[15] W. E. van der Veer, R. J. J. van Diest, A. Donszelmann, and H. B. Linden van den Heuvell, Phys. Rev. Lett. **70**, 3243 (1993).
[16] A. Lezama, Y. Zhu, M. Kanskar, and T. W. Mossberg, Phys. Rev. A **41**, 1576 (1990).
[17] A. Imamoglu, J. E. Field, and S. E. Harris, Phys. Rev. Lett. **66**, 1154 (1991).
[18] Y. Zhu, Phys. Rev. A **45**, R6149 (1992); **47**, 495 (1993); Y. Zhu, O. C. Mullins, and M. Xiao, *ibid.* **47**, 602 (1993).
[19] M. Fleischhauer, C. H. Keitel, M. O. Scully, C. Su, B. T. Ulrich, and S. Zhu, Phys. Rev. A **46**, 1468 (1992).
[20] C. Cohen-Tannoudji, in *Frontiers in Laser Spectroscopy,* Proceedings of the Les Houches Summer Schools, Session XXVII, edited by R. Balian, S. Haroche, and S. Liberman (North-Holland, Amsterdam, 1977).